



Nicolas PAILLET

COURSE Physics & NanoScience (PNS)
Academic year 2014-2015

INTERNSHIP REPORT

FABRICATION AND MEASUREMENTS OF NIS JUNCTIONS TO CHARACTERIZE PLASMA ETCHING

Internship realized from the 18th of May 2015 until the 18th of August 2015

Within the PICO GROUP



Under the supervision of

Professor Jukka PEKOLA, as internship tutor
jukka.pekola@aalto.fi
&
Quentin RAFHAY, as school tutor
quentin.rafhay@phelma.grenoble-inp.fr

Confidentiality : No

AKNOWLEDGMENTS

First of all, I would like to thank Pr. Jukka Pekola for having accepted me within the PICO Group and having given me the possibility to do this internship. Of course this would not have been possible without Dr. Clemens Winckelmann who gave me Pr. Pekola contact details. Then, I will of course thank the whole PICO Group for having integrated me so well and helped me when I needed it, but especially Dr. Mathieu Taupin who I worked with on plasma etching project and who gave me precious advices about clean room processes and laboratory methods, alongside with Dr. Matthias Meschke on that last point. Finally, I would like to thank both GRENOBLE INP PHELMA for having given me the opportunity to do such an internship and Aalto University which made it possible afterall.

Contents

Glossary	1
List Of Figures	2
The PICO Group	3
Introduction	4
1 Theory	5
1.1 Superconductivity	5
1.2 NIS Junction	6
1.3 Leakage current	6
2 Experimental methods	8
2.1 Resists	8
2.2 Electron Beam Lithography and development	9
2.3 Evaporation	10
2.4 Lift-off and Scanning Electron Microscope	11
2.5 Dilution cryostat	13
3 Experimental protocol	17
3.1 Parameters	17
3.2 Experimental procedure	17
3.3 Oxygen cleaning	18
3.4 Measurement setup	18
4 Results and discussions	20
4.1 Room Temperature Results	20
4.2 Low temperature measurements	23
4.3 Summary of the results	26
Conclusion	28
A Specification about experimental methods	30
A.1 Chemicals	30
A.2 EBL schematics	31
B Parameters table of the samples	32
C Gantt Diagramm	33

Glossary

BCS theory : Theory of superconductivity as explained by Bardeen, Cooper and Schrieffer

DOS : Density of electronic states

EBL : Electron Beam Lithography

IVC : Isolated Vacuum Chamber

LISA : Nickname of one of the evaporator in Aalto Nanofab

MIBK : Methyl IsoButyl Ketone, a developper

MMA : Methyl Methacrilate, a resist

NIS junction : Normal metal – Insulator – Superconductor junction

PMMA : PolyMethyl Methacrilate, a resist

List of Figures

1.1	Schematics explaining the formation of Cooper pairs	5
1.2	Density of states for different V_{bias} for a NIS junction	6
2.1	Spinning + Baking	8
2.2	Cross-section view after resist deposit, spinning and baking	9
2.3	Electron Beam Lithographier Vistec of Micronova cleanroom	9
2.4	Cross-section view after EBL	10
2.5	Cross-section view after MIBK (full lines), and after MethyGlycol (dotted lines)	10
2.6	Picture of the LISA evaporator in Micronova cleanroom	11
2.7	Cross-section during evaporation	12
2.8	Scanning Electron Microscope	12
2.10	Phase diagram of ${}^3\text{He}/{}^4\text{He}$ mixture	14
2.11	Pictures of the preparation of the sample stage	15
2.12	Pictures of the cool down	15
2.13	Dilution fridge functioning schematics	16
3.1	Pattern of the junctions	18
3.2	Four-probe measurements schematics	19
4.1	Resistance of clean contact in function of the surface area	21
4.2	Conductance in function of surface area for a strong oxidized sample	21
4.3	Conductance in function of surface area for a tunnel junction sample	22
4.4	Resistance in function of surface for different positions of the samples on the LISA's sample stage	23
4.6	SEM Image of a sample where the wafer was etched by plasma	24
4.8	Evolution of the IV curves of a NIS junction with the temperature	26
4.9	IV curves of Plasma Etched sample	27
4.10	IV curves of the reference oxidation sample	27
A.1	Chemical structure of MMA, PMMA is a polymer made of this monomer .	30
A.2	Chemical structure of MethylIsoButylKetone (MIBK)	30
A.3	Simplified EBL functional diagram	31

The PICO Group

The PICO Group is a research team which works under the responsibility of the Aalto University School of Science. Its facility lies in the Micronova building, situated on the Aalto Campus of Otaniemi, in Espoo, Finland. Otaniemi is the centre of all scientific activites of the Aalto University and the Micronova building holds a major part of research about nano and microphysics in Finland. The PICO Group consists of nineteen members for the moment, including, professor Jukka Pekola, who leads the group, and doctor Matthias Meschke, in charge of the laboratory. Then, the group is divided between five post-doc, seven PhD students and five summer students.

The main topics are quantum thermodynamics and single electron transport through nano and microscaled devices. The topics studied are both on the experimental and theoretical sides. The group focuses for example on the theory of heat transfert between two nanoscale resistors[1] or the practical realization of electron counting devices. Moreover, the group works actively with the Centre for Metrology and Accreditation (MIKES) because one of their goal is to redefine the ampere, the unit used to measure electrical current and still missing in a metrological point of view (measurements not accurate enough so far)[2].

The practical realization of the different devices is possible thank to the presence in the building of an cleanroom with a classification from ISO6 to ISO4. A large panel of equipments is available, but for the project of the intership, only two Scanning Electron Microscope (SEM), one for imaging and one equipped with Electron Beam Lithography (EBL), and an evaporator for metal deposition will be needed. The cleanroom also holds devices for making semiconductors-based structures and the Atomic Layer Deposition device was invented here. The group has a low temperature laboratory with several dilution cryostats. Indeed, since the thermal agitation should be smaller than the characteristic energies of the mesoscopic system (superconducting gap, charging energy... typically \sim meV), they need to reach low temperatures[3]. There are three dilution cryostats that can reach a temperature of 50mK, and a BlueFors dry cryostat which works without Helium bath, reaching 10mK. Other characterization equipments are present, such as a probe station, or an Atomic Force Microscope.

The University and these devices provide the Group the possibility to make research efficiently as we can see the numerous publications published every year in famous journals.

Introduction

Research in microstructures is very active since it provides a way to understand the properties of matter at atomic scale which gives access to numerous applications, such as transistors or detectors. Results in this field may offer new possibilities for the future, in research and also in everyday's life. But, in order to make microstructures, a research group needs several devices for which we know the functioning. Indeed, having a device with a large amount of functionalities is important but knowing how all these functionalities work is more important. When a device is new in a laboratory, the first step is to characterize each functionality to be sure of the behaviour of the tool.

The evaporator, surnamed LISA, is a recent acquisition in Micronova's cleanroom, so that all its functionalities were not characterized, for example it allows plasma etching, which is an *in situ* etching that can be used to get rid of a layer of matter that is not wanted on the structure. There are other etching methods, like chemical etching but these are *ex situ*, meaning that the etched surface can get contaminated during the transport from one instrument to another. For example, Aluminium is a metal that oxidizes very fastly (few dozens of second) in contact with air, getting rid of Al oxide with an *ex situ* method is not worth since at the second the sample will be in contact with air, it will oxidize again.

Before using plasma etching on real samples, and as it is a new technique, it is important to characterize it : is the plasma uniform on all the sample holder, does it affect the quality of the junction ? In order to answer these questions, we will study simple structures : Normal metal-Insulator-Superconductor junction (NIS junction).

The report is divided as follow. First of all, a theory part will sum up the literature to situate the state of the art and remind the main characteristics of the devices (Chapter 1).

Then, we will focus on the experimental tools that were used to make the structures : the goal of this part is to present the functioning of all the devices useful for the process, to show why each step is important and start to define the parameters that need to be set (Chapter 2).

With this knowledge of the tools, we can build an experimental procedure to characterize the plasma : several parameters for the fabrication, consistents and relevant measurements, and design of the measurements (Chapter 3).

Finally, the last part will focus on the results of the measurements, and the exploitation of these results that allows to draw conclusions about plasma etching (Chapter 4).

Chapter 1

Theory

In this chapter we will describe the principle of superconductivity and equations that rule NIS junctions.

1.1 Superconductivity

Superconductivity is a state of matter which occur at low temperature for several materials. It is a state where the material have an absolute zero resistance, so that current can run without energy losses and where the material totally excludes magnetic field and becomes perfectly diamagnetic[4]. The theory of superconductivity has been established by Bardeen, Cooper and Schrieffer in 1957, and is known as the BCS Theory[5].

The idea of the BCS theory is that electrons can pair in so-called Cooper pairs which come from the interaction between electrons and the ion lattice, the phonons. At low temperature, electrons are slow and they tend to attract ions. These ions have a relaxation time to come back to their initial state, but during the time they are in a non-equilibrium state, they create a local positive charge (See Fig. 1.1) that can attract another electron from somewhere else (10^3 the ion lattice characteristic distance) in the matter. This electron is then paired with the previous one. It has the opposite wave vector and an opposite spin according to the BCS Theory. In the superconducting state, the Cooper pairs form a condensate at the Fermi energy, and a consequence is the formation of a gap in the density of states (DOS).

The electronic density of states follows the following rule (Eq. 1.1), with N_0 the normal

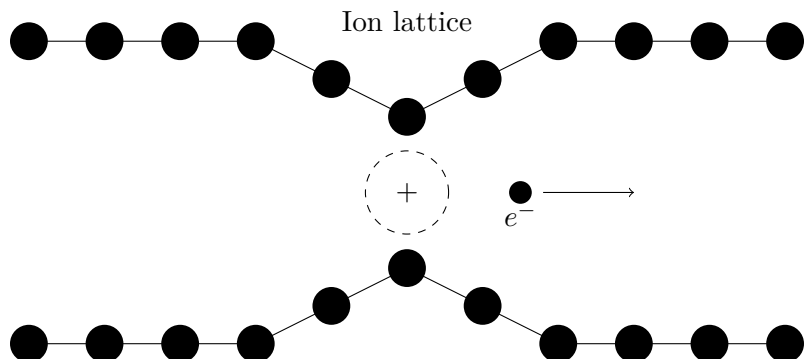
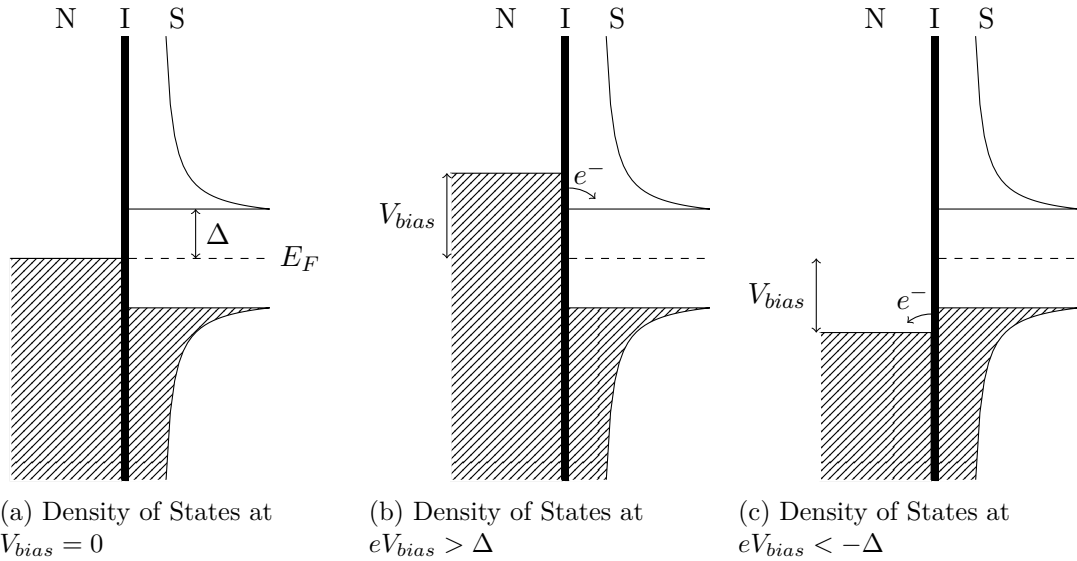


Figure 1.1: Schematics explaining the interaction between electrons and the ion lattice. In a superconductor, the positive area attracts another electron from elsewhere in the matter


 Figure 1.2: Density of states for different V_{bias} for a NIS junction

DOS and Δ the superconducting gap.

$$N(E) = \begin{cases} N_0 \frac{E}{\sqrt{E^2 - \Delta^2}} & \text{if } |E| > \Delta \\ 0 & \text{if } |E| < \Delta \end{cases} \quad (1.1)$$

1.2 Normal Metal-Insulator-Superconductor Junction

In the case of a Normal Metal-Insulator-Superconductor (NIS) Junction, we make a contact between materials with different density of electronic states, as shown in Fig. 1.2a. The DOS of a normal metal is constant at the Fermi energy and for a superconductor, it follows the previous equations. Applying a voltage will translate these densities of states. While $|eV| < \Delta$ (subgap regime), electron cannot tunnel through the insulator as there is no states available in the superconductor, but as soon as $|eV| \geq \Delta$ (ohmic regime), they can start to tunnel in one direction or the other depending on the sign of the bias voltage as shown in Fig. 1.2b and Fig. 1.2c[6]. It has to be noted that in principle the tunneling of a Cooper pair is possible in the region $|eV| < \Delta$, but this process is less probable (second order tunneling) and we will neglect it.

The current that crosses the NIS junctions is where f is the Fermi-Dirac distribution, and g the density of states.

$$I(V) = \frac{1}{2e} \int d\varepsilon g(\varepsilon) [f(\varepsilon - eV) - f(\varepsilon + eV)] \quad (1.2)$$

1.3 Leakage current

In practice, the junctions are not perfect and electron tunneling can be induced by some impurities or by interaction with photon. To take into account these unwanted tunneling processes, we introduce the Dynes density of states [7]. It is a broadening of the DOS written in the BCS theory with a linewidth parameter Γ :

$$N = Re \left(\frac{|E| + i\Gamma}{\sqrt{(E + i\Gamma)^2 - \Delta^2}} \right) \quad (1.3)$$

This new DOS induces a small current in the subgap regime. So there can be tunneling within the gap since the DOS is not equal to zero, however very limited. The resulting current is called leakage current and shows, among other things, the defaults of the junction. The leakage is defined as the ratio between the resistance in the ohmic regime (R) and the resistance in the subgap regime (R_{leak}). A junction is generally considered as good if :

$$\frac{R}{R_{leak}} < 10^{-4}$$

Chapter 2

Experimental methods

Tools and experimental methods provide the ways to make structures. In this part we will see how the devices and methods used for the process work. In the last part we will talk about the dilution cryostat which was used to cool down samples.

2.1 Resist

The first part of the process is the deposition of resists on a Silicon wafer with a layer of SiO_2 .

The resists we use consists of polymer materials : Polymethyl Methacrilate (PMMA) and Methyl Methacrilate (MMA) (See Appendix A.1 Fig. A.1). PMMA is a polymer made out of MMA. We deposit the resists on the top of the wafer and then a spinner rotates the wafer and makes a thin and uniform layer of resist, with a thickness from 100nm to 500 nm depending on the rotation speed and the type of the resist. In our case, the copolymer thickness is around 400nm.

Practically, we use these two types of resists because they have a different reactivity to the e-beam lithography and to the development process. These two layers have different thicknesses since they do not have the same role. PMMA acts as a pattern designer, so it can be thin ($\sim 100 - 200\text{nm}$), whereas we will dig the MMA to create undercuts where the metal will be deposited in the evaporator, this is why the MMA layer needs to be thicker ($\sim 1.2\mu\text{m}$), to avoid evaporating on the undercut. Then the resists are baked with a hot plate. The datasheet of the resists can be found in Ref. [8]. We finally obtain the cross-section shown in Fig. 2.2.

The resists we use are sensitive to electrons with a particular energy, what we will do next is to expose the resist to an electron beam (See 2.2.1) which will imply structural modifications. The electrons break the polymer into smaller pieces, which make the exposed resist more soluble in Methyl IsoButyl Ketone (MIBK) (See 2.2.2).

Other type of resists exists, especially some resists damaged by light (photoresists), which are mostly used for semiconductors-based structures.

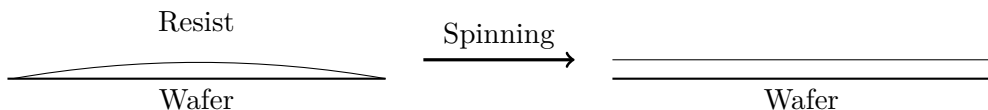


Figure 2.1: Spinning + Baking

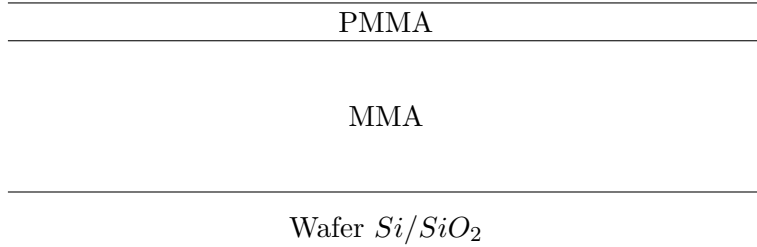


Figure 2.2: Cross-section view after resist deposit, spinning and baking



Figure 2.3: Electron Beam Lithographier Vistec of Micronova cleanroom

2.2 Electron Beam Lithography and development

Once the wafer have been prepared and is covered by resists, we can draw a pattern in these resists, with the Electron Beam Lithography (EBL).

2.2.1 Electron Beam Lithography

The EBL is a tool which is used to design the patterns we want to have for our structures[9]. It sends an electron beam onto the resist to damage the bonds of the resist, making the exposed area sensitive to the development process. The functionnal diagram can be found in Appendix A.2 Fig. A.3. The E-beam lithography gives the opportunity to make very small structures, down to few tens of nanometer in size with a resolution of few nanometers. The drawback of such low resolution is the writing time, a compromise between good accuracy and reasonable writing time has thus to be found.

For example, the only part that requires an good accuracy in our process is the junction, so we have to use a good resolution there, but for the leads, which are much larger when the actual size does not matter, so we can choose to go faster. In addition to the primary electrons from the beam, the resist is also affected by the secondary elestrons, backscattered from the substrate. These electrons will create a wider exposed area below the PMMA and is called "undercut" (See Fig. 2.4). This is this undercut that give the possibility to shadow evaporation (see below).

Once the wafer has been exposed, it can be represented by Fig 2.4.

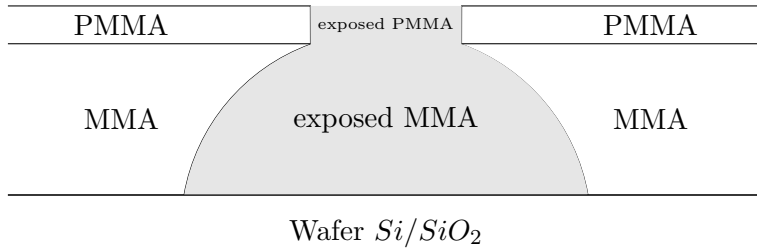


Figure 2.4: Cross-section view after EBL

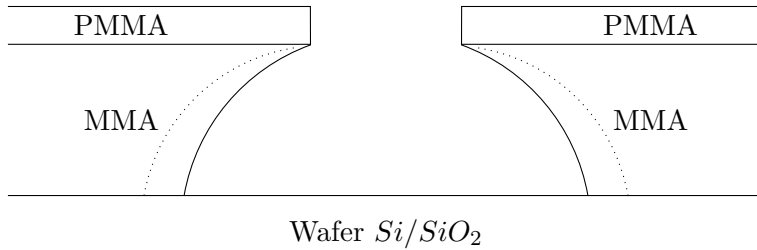


Figure 2.5: Cross-section view after MIBK (full lines), and after MethyGlycol (dotted lines)

2.2.2 Development

The Development consists in the withdrawal of the exposed resist. It is realized by chemical reactions.

The MIBK(See Appendix A.1 Fig. A.2) will dissolve fastly the exposed PMMA and MMA (Fig. 2.5).If we want to increase the width of the undercut, it is possible to add an extra step and to use MethylGlycol after the development in MIBK. The MethyGlycol can dissolve MMA and thus increase the undercut [10]. This is particularly useful if we want to work with large angles.

There, we can see that if we depose metal with a certain angle, they will overlap only in the chosen area. Finally, we dive the sample in Isopropanol to stop the reaction.

The dissolution will depend on the time we dive the samples into the chemicals, we need to chose this time considering the width of the undercuts but ensure that PMMA does not collapse.

2.3 Evaporation

During the evaporation step, we make the junctions by evaporating metal.

2.3.1 Functioning of evaporator

The evaporator is a tool that allows to deposit a uniform, thin layer of metal. A filament is submitted to a large tension (10kV) and current, it emits electrons that are deflected with a magnetic field to focus on a crucible which contains metal. The metal will melt, or even sublimate, depending on the metal. The atoms can move without collision in the very low pressure chamber ($P \sim 10^{-7} mbar$) : the mean free path is longer ($\sim 1km$) than the distance between the crucible and the sample holder ($\sim 50cm$). The deposition of the atoms is very uniform and the thickness is measured with capacitive sensors. The chamber of the evaporator is connected to a pure Oxygen line, in order to perform oxidation *in*



Figure 2.6: Picture of the LISA evaporator in Micronova cleanroom

situ. The most common superconductor used is Al, and its oxidation is very rapid (an exposure of 2mbar of O₂ during 2 minutes is enough to create a tunnel barrier).

2.3.2 The Plasma gun

The evaporator is also equipped with a Plasma Gun, with Argon valve. The plasma is mostly used at low power to ease the lift-off (See 2.4.1) by weakening the resist and to clean the surface. But with the accurate parameters it can also be used for etching. The idea of plasma etching is to etch native oxide of a material, which has been grown in another process, so exposed to air, and to make contact in a controlled way (clean contact or tunnel barrier).

2.3.3 Evaporator in action

The Fig. 2.7 shows the principle of evaporation. First, we deposite the first layer of metal with a previously determined angle. If needed, it is possible to oxidize to obtain a tunnel barrier, then another layer is evaporated, with another angle. The pattern and the angles are such that only the active parts (the junctions) will overlap. Thus, we can see that even if they are in the same undercut, they do not touch each other. To make the junction, we have to have two different undercuts that overlap.

2.4 Lift-off and Scanning Electron Microscope

2.4.1 Lift-off : resist withdrawal

The lift-off is a process where the resist is removed to get our final structures. The chip is dived into an acetone bath, which will dissolve the resist and left on the substrate only the device made.

2.4.2 Scanning Electron Microscope

The functioning of Scanning Electron Microscope (SEM) is very similar to the EBL one, since actually, SEM and EBL are the same instrument, except that this time we do not want to weaken the matter but to observe the scattering of electrons within it. This allows us to check if the junctions made looks measureable, if metals evaporated overlap in the chosen area, meaning that the angle is correct. It is useful for a process that is

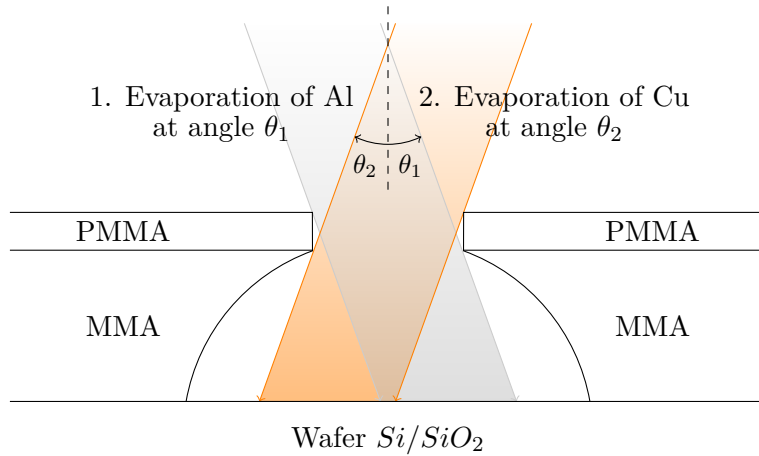


Figure 2.7: Cross-section during evaporation (the two metal are evaporated successively, not at the same time)



Figure 2.8: Scanning Electron Microscope

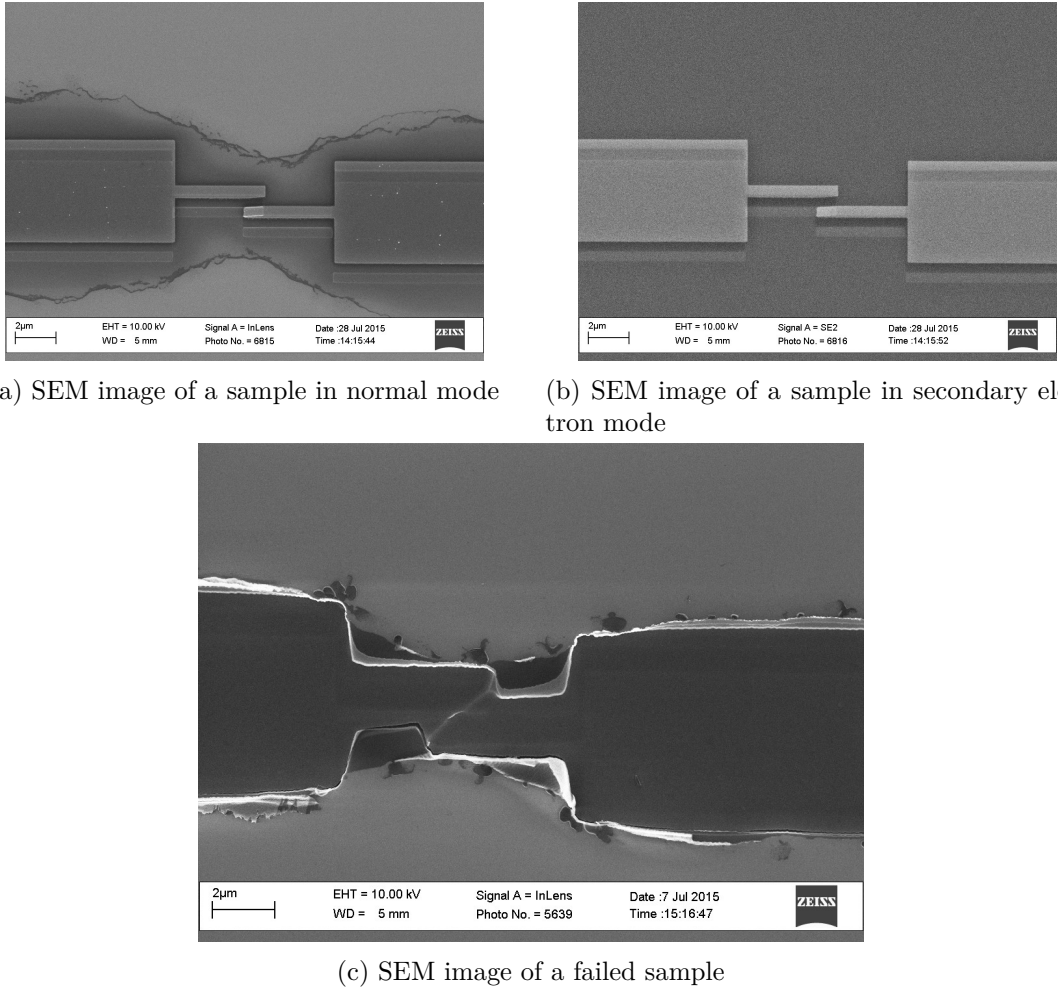
not completely established, where the angles, or the EBL electron dose are still to be improved.

2.4.3 Observation of the samples

The SEM is very similar to an optical microscope, in the way that the clarity of the image will depend on the focusing of the beam on the sample, except that it is not light here but electrons. This can be problematic as it can be possible to charge the objects observed if the beam stays too long on the same spot, and this can damage the junctions, especially if they are small.

As in the EBL, the matter scatters the electron, especially metals. These scattered electrons can be detected with the secondary electron mode. Since each metal scatters electrons in a different way, in this mode will only the metals appear and different contrasts allow to distinguish them, despite the brightness and quality of the signal (few scattered electrons inducing noise).

A typical SEM image is shown in Fig. 2.9a and an image with the secondary electron mode of SEM is shown in Fig. 2.9b. As said before, the SEM can show some problems with the junctions, like in Fig. 2.9c. In our case, a chip contains 20 devices. It is not necessary to image all of them, only a few are sufficient, as the real test to determine the



quality of the device is the measurement of the resistance.

2.5 Dilution cryostat

2.5.1 Cooling theory

The ^4He is liquid at a temperature of 4.2K. The minimum reachable temperature with ^4He is 1.2K and 0.3K for the ^3He by pumping. In order to reach lower temperatures, we use a mixture of $^3\text{He}/^4\text{He}$, where the temperature can be as low as 3mK in the best fridges. The phase diagram of the $^3\text{He}/^4\text{He}$ mixture is shown in Fig. 2.10 : with 10-15% of ^3He , a phase separation will occur below 0.5K due to the existence of a "forbidden zone" in the diagram. We will thus have a rich phase (of ^3He) and a diluted phase.

The whole cooling power lies in this phase separation [11]. The mixture goes through a 77K nitrogen trap, in order to be cleaned of any impurities, then a line run through the fridge towards the ^4He bath at 4.2K then to a 1K pot (pumped ^4He bath). This bath liquefies the mixture which then goes to an exchanger, the still that cools down to 600mK, and ends up in the mixing chamber where the phase separation occurs which has for effect to remove heat from the mixing chamber environment. The mixture is pumped back out of the fridge and injected again through the condensing line, as a close loop.

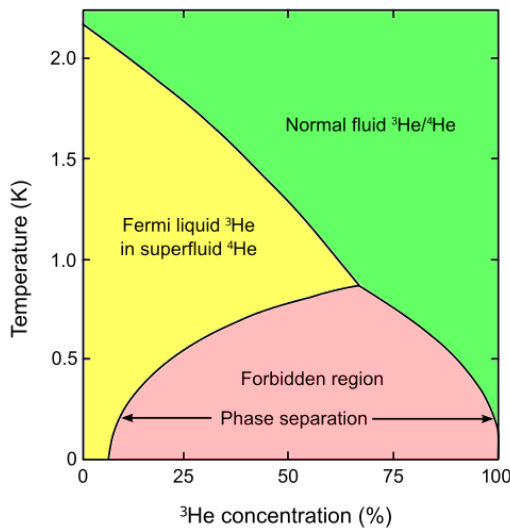


Figure 2.10: Phase diagram of ${}^3\text{He}/{}^4\text{He}$ mixture

2.5.2 Preparation of the sample

The first thing to do with low temperature measurements is to prepare the sample to get in the fridge. Sample holder consists in metallic pads linked to a 12-pins connector. The sample is bounded to the sample holder with thin Al wires with an ultrasound bounder (Fig. 2.11a). The sample holder is screwed to the fridge (Fig. 2.11b) and sealed in the vacuum chamber (IVC).

2.5.3 Cooling down

The first step of the cooling is to pump the Isolated Vacuum Chamber (IVC) to remove all the air from it and avoid any freezing. Then, some exchange gas (Helium) is inserted into the dilution, in order to reduce the thermal conductivity that exists between the stages of the fridge. The gas will cool down the dilution by convection. The fridge is then placed in a nitrogen bath (Fig. 2.12a) during approximatively thirty minutes before diving it in the Helium dewar. The goal is to avoid to evaporate Helium in the dewar (the difference between 77K and 4K is less important and Nitrogen can be cooled more easily). Once the fridge is thermalized at 4K (Fig. 2.12b), checked by RuO_2 thermoresistor, the exchange gas is pumped back to avoid heat transfert by convection, otherwise the fridge can not be cooled down to 50mK. Finally, the mixture is inserted in the fridge and starts to circulate, like in Fig. 2.13



(a) Picture of the sample stage



(b) Exchanger and mixing chamber with the sample holder

Figure 2.11: Pictures of the preparation of the sample stage



(a) Picture of the IVC dived into liquid nitrogen



(b) Picture of the setup when the fridge thermalize at 4.2K

Figure 2.12: Pictures of the cool down

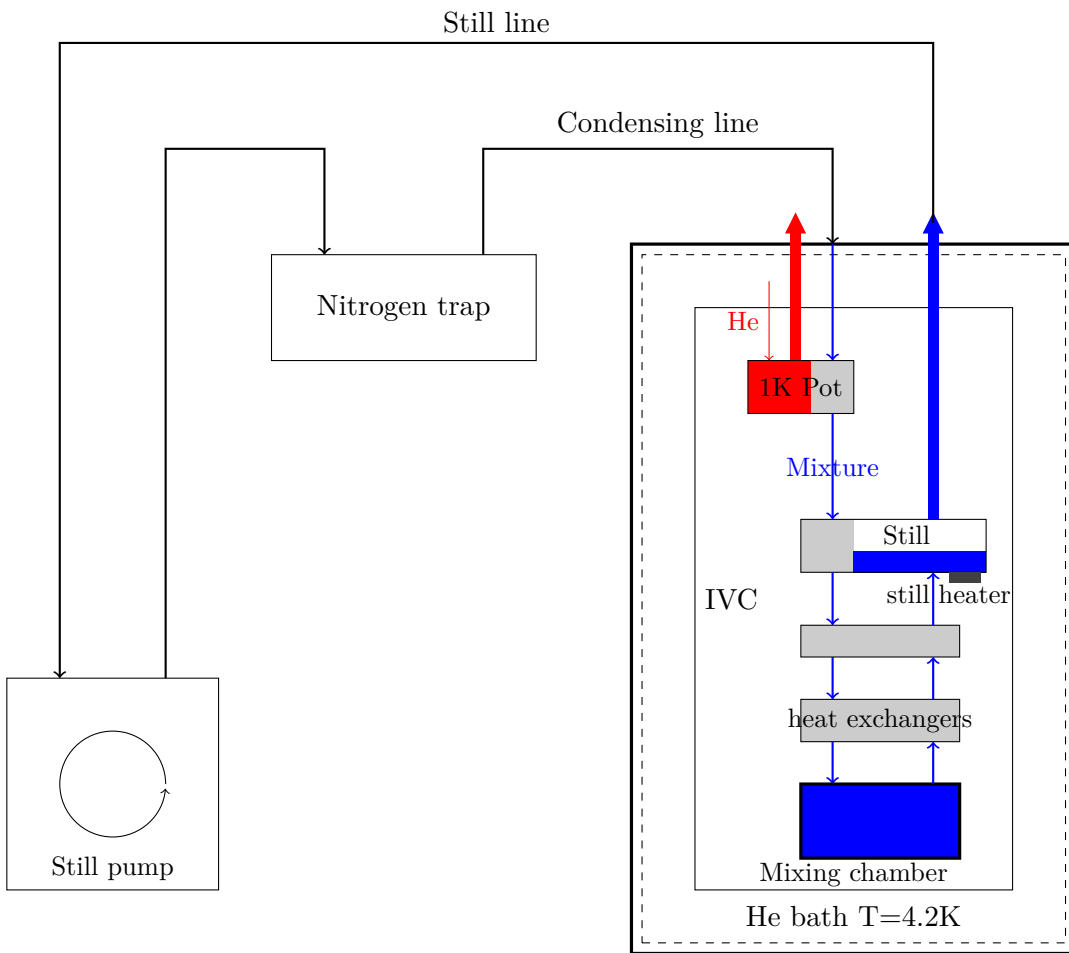


Figure 2.13: Dilution fridge functioning schematics : The still pump and the nitrogen trap are outside the dewar. The mixture that is injected in the IVC is represented in blue, the ^4He is in red. The grey parts are heat exchangers

Chapter 3

Experimental protocol

In this part, we will describe the experimental protocol that was used for the realization of the structures and the setup for the measurements made.

3.1 Parameters

The following table describes the different tools used for the realization of the samples and shows the main parameters that have to be taken into account during the fabrication. The parameters in bold are the most influent.

STEP	DEVICE	PARAMETERS
Resist deposition	Spinner	Rotation Speed, Acceleration, Time
Resist baking	Hot plate	Temperature, Time
Pattern design	EBL	Dose, Shape(area), Resolution
Development	MIBK, MG, IPA	Duration, Concentration
Deposition of metal	Evaporator	Angle
Oxidation	Evaporator	Pressure, Duration
Plasma Etching	Plasma gun	Duration, Position, Power
Lift-off	Aceton	\emptyset

Table 3.1: Steps of the process, tool or method used to realize this step and parameters involved by the step

The chip realized consists in twenty samples, with four different surface areas. It is thus possible to make a small statistic for the room temperature measurements.

3.2 Experimental procedure

Here is the experimental procedure of the process. Based on 4 layers of MMA and one layer of PMMA and EBL dose from 2000 to 3000 $\mu\text{c}/\text{cm}^2$, according to the pattern in Fig. 3.1, the chip was dived 20s in MIBK, 20s in MG and IPA, to develop the exposure. In the evaporator, 20nm of Al are evaporated. To reproduce the native oxidation when exposed to air, the Al can be strongly oxidized with a pressure of 200mbar of O₂ during 10 min. After the strong oxidation, plasma etching is performed *in situ* to get rid of the thick oxide layer. The tunnel barrier are made by exposition to O₂ at a pressure of 2mbar

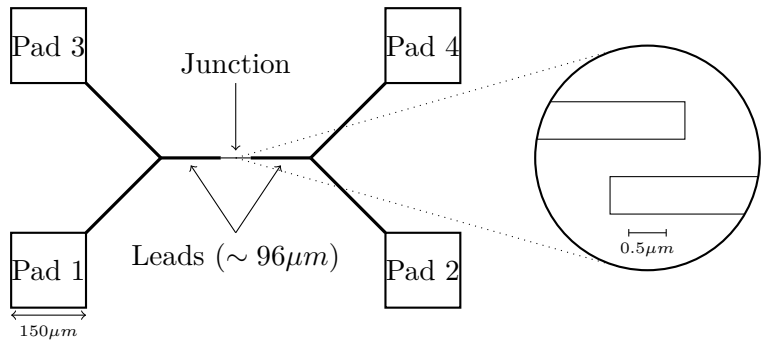


Figure 3.1: Pattern of the junctions

during 2min. Finally, 25nm of Cu are evaporated before diving the sample in acetone for the lift-off. In order to test the plasma etching, several realizations have been done, first to get some references (without plasma etching) :

- Clean contact
- Strong Oxidation
- With tunnel barrier

Then we made samples with strong oxidation, then plasma etching, and finally either clean contact or with a tunnel barrier. An exhaustive table of the parameters used for each test can be find in Appendix B. Both room temperature and low temperature measurements are done, their goal are different. Room temperature measurements allows to check if the plasma really etches : the resistance of the samples should be similar to the resistance of reference samples. The low temperature measurements give us the quality of the junctions, especially the difference of quality between plasma etched samples and reference samples, which is not possible at room temperature.

3.3 Oxygen cleaning

After heavy use of the plasma for etching, some troubles appeared and a cleaning of the gun with plasma oxygen was needed. After the cleaning, the etching power of the plasma seemed to have increased, and whereas ten minutes of plasma was needed in the first runs, the same etching time over-etches the sample after the oxygen cleaning (See Chapter 4) and it has thus to be reduced.

3.4 Measurement setup

3.4.1 Room temperature setup

Four-probe resistance measurements were realized thank to a probestation. The four-probe measurements make sense as it is the only way to measure the real resistance of the device, without parasite resistances (pads, wires). A schematics representing four-probes measurements is shown in Fig. 3.2. The probestation applies a voltage with an electrode and makes a slope from -100 mV to 100 mV, but measures the voltage V_{sample} and the current i_{sample} with two other electrodes so, the voltage and current measured are really these that cross the sample. The linearization of the I-V curve obtained directly gives the resistance of the sample, which is made through a matlab program.

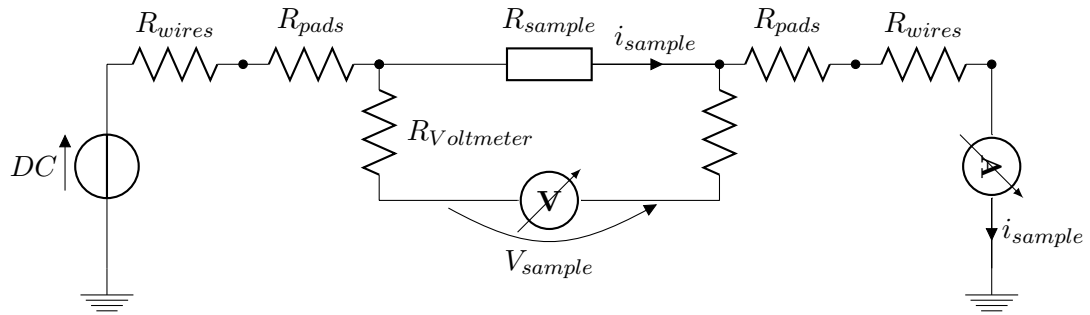


Figure 3.2: Four-probe measurements schematics

3.4.2 Low temperature setup

Measuring samples at low temperature is necessary to completely characterize the samples. First, it allows us to reach the superconducting state of Al ($T_C=1.2K$). Then, it reduces the thermal energy $k_B T$ so it reduces thermic transport which widen the electronic transitions. The samples are measured with two probes and not four like at room temperature. There are two main reasons, first the important parameter we want to get is $\frac{R}{R_{leak}}$ to check the quality of the junction, and this parameter will not be very affected by parasite resistance, since it is measured in order of magnitude : R_{leak} is order of magnitudes higher than parasite resistances. Secondly, it is important to have some statistics, and the number of samples bounded for each cool down is limited, we thus make the choice to have statistics rather than few very accurate results. The measurements made are I-V curves with adjustements for the range of V_{bias} : a large range for the tunnel current and a small range for the leakage current.

Chapter 4

Results and discussions

This part will present the results the measurements gave and the discussions we can have give according to these results.

4.1 Room Temperature Results

4.1.1 Reference Samples

Every experiment needs references to rely on. Before starting anything with the plasma, it is important to know the behaviour of the same structures (in terms of parameters) without plasma, to have access to a comparison. The three reference samples are a clean contact (Al/Cu), a strong oxidation reference (as a native oxidation imitation) (Al/Al Oxide/Cu) and a tunnel junction (Al/Al Oxide/Cu).

The first junction is a clean contact with only Al and Cu as a reference. Since the contact is clean, the resistance of the interface between the two metals should be negligible, then the resistance we measure is :

$$R = \sum_{Al,Cu} \frac{\rho L}{S} \quad (4.1)$$

The resistance does not depends on the surface area of the junction, as you can see in Fig. 4.1 the results of four probes measurements. As expected the resistance does not depend on the resistance of the surface of the junction. The theoretical calculus from this law with the parameters used gives 78Ω , which is close to the value we find. There are some uncertainties : the thickness of the metal is not very precise, the dimensions of the device can differ a bit from the pattern dimension. However, the order of magnitude is correct, so our reference for the leads resistance is around 70Ω .

After the clean contact, the second reference sample is with a strong oxidation (10 min at an oxygen atmosphere of 200mbar).

For the NIS junctions, it is more relevant to draw conductance in function of the surface area of the junction. Indeed, the previous law (Eq. 4.1) is correct for an insulator, except that ρ_{AlOx} is order of magnitudes higher than ρ_{Al} or ρ_{Cu} and the surface of the junction is the surface of the insulator considered. The resistance of the device is mostly the resistance of the junction, and the conductance of the junction is linear with the surface. The measurements on these samples gave the conductance curve represented in Fig. 4.2 where :

$$\frac{1}{R} \propto S$$

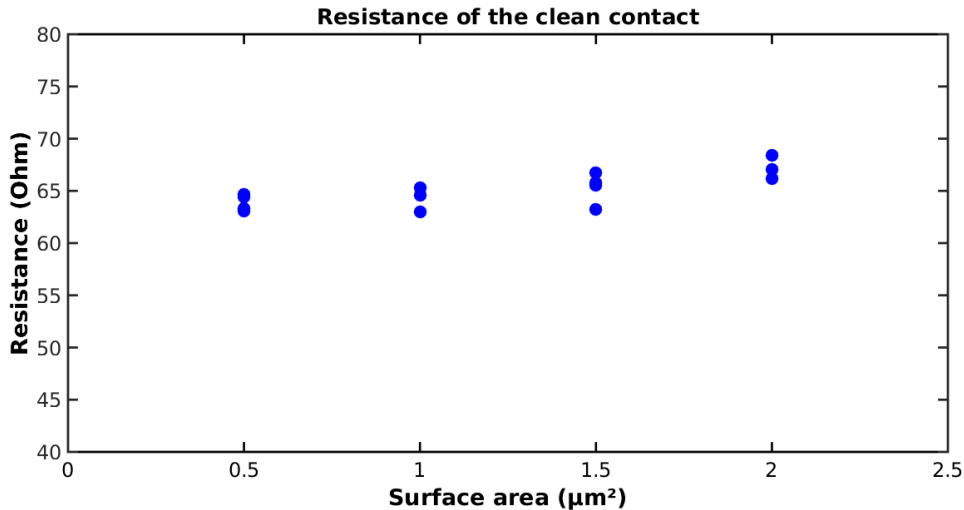


Figure 4.1: Resistance of clean contact in function of the surface area

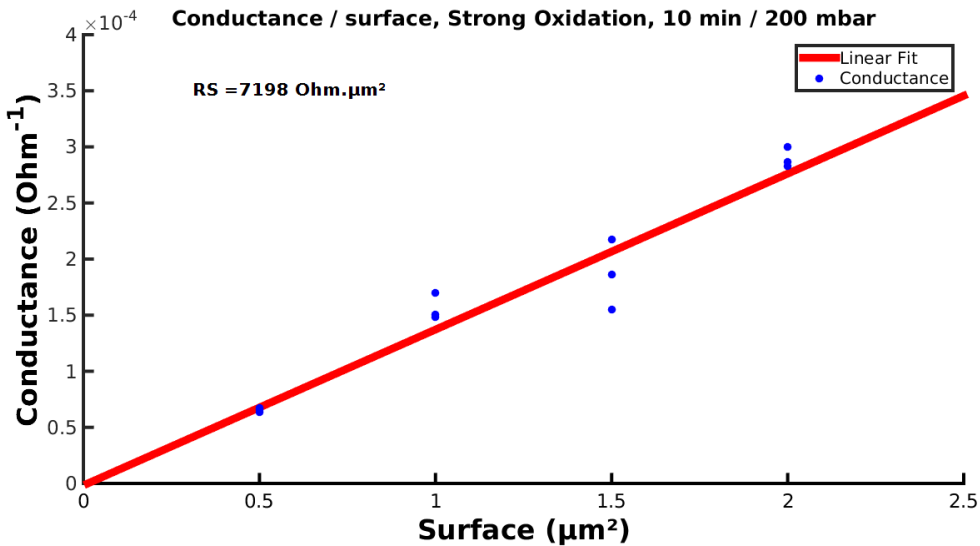


Figure 4.2: Conductance in function of surface area for a strong oxidized sample

We can extract a parameter from the slope :

$$RS = 7.18 k\Omega \cdot \mu\text{m}^2$$

This parameter is linked with the thickness of the oxide layer.

In order to cover a large range of resistance, the third reference sample is also a tunnel junction but lighter than the previous one (2min at an oxygen atmosphere of 2mbar).

Again, it is more relevant to draw the conductance (See Fig. 4.3) to determine the RS parameter.

$$RS = 763 \Omega \cdot \mu\text{m}^2$$

RS is ten times less important than for the strong oxidation. It means that the oxide layer is quite thinner in this case, which is normal since the Al was less oxidized in this

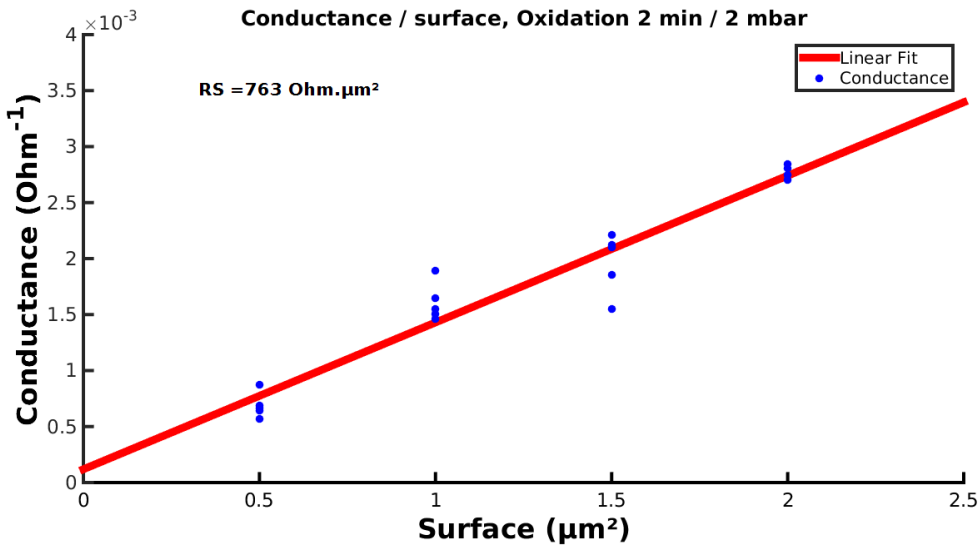


Figure 4.3: Conductance in function of surface area for a tunnel junction sample

case. These three references give us a base to evaluate the quantity of oxide we etch when we use the plasma.

4.1.2 Plasma Etching : Position of the sample

The first test to do with the plasma etching is to determine if the beam is focused on the whole sample stage (15cm diameter) and not only on the center. This information will ensure a good homogeneity of the etching on all the surface. In order to do so, four samples were placed on the sample holder : one in the center and three on the side (see inset of Fig. 4.4). The layer of evaporated Al was strongly oxidized, then the oxidation layer was etched by argon plasma for 10 min. Finally, we have made a clean contact by evaporating Cu. The Figure 4.4 shows the results of these tests. We can see that the position does not affect the resistance of the sample so we can assume that the etching is quite uniform. And another conclusion of this graph is that 10 min of plasma are enough to etch all the Al oxide : there is no surface dependance like for the oxidized samples and the resistance is about the same order of magnitude than the clean contact junction. The value is a bit higher because the plasma etches the oxide, so the Al layer is thinner (since AlOx is not deposited on top of Al), which reduces the surface section of the lead, thus, it increases the resistance.

4.1.3 Time of plasma etching

The time during which the sample is exposed to the plasma is important and determines how much material will be etched and implicitly the resistance of the sample. The process is the same for all the samples, only the etching duration is modified. The Figure 4.5a shows the resistance compared to plasma etching duration before the cleaning of the plasma gun. We can see that there is not a lot of differences between 10 and 20 minutes but the most relevant result is what we can see on the Figure 4.5b, with samples made after the cleaning, it seems that less than 5 minutes are enough to etch all the oxide, since the results are very similar, yet for totally different duration times. It means that the cleaning had an effect on the plasma behavior.

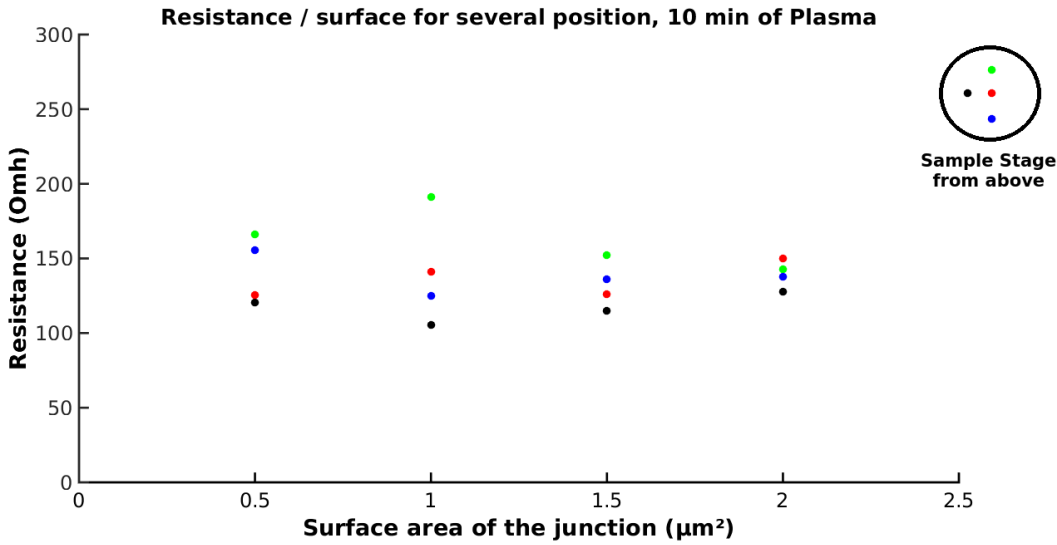


Figure 4.4: Resistance in function of surface for different positions of the samples on the LISA's sample stage

4.1.4 Wafer Etching

According to the previous results, we can think that the oxygen cleaning made the plasma gun more powerful. Here is an observation that confirms this. The Figure 4.6 shows a SEM image of a sample exposed 10 minutes under the plasma after the oxygen cleaning. We can see that the plasma created a hole in the wafer, before the deposition of the copper above it.

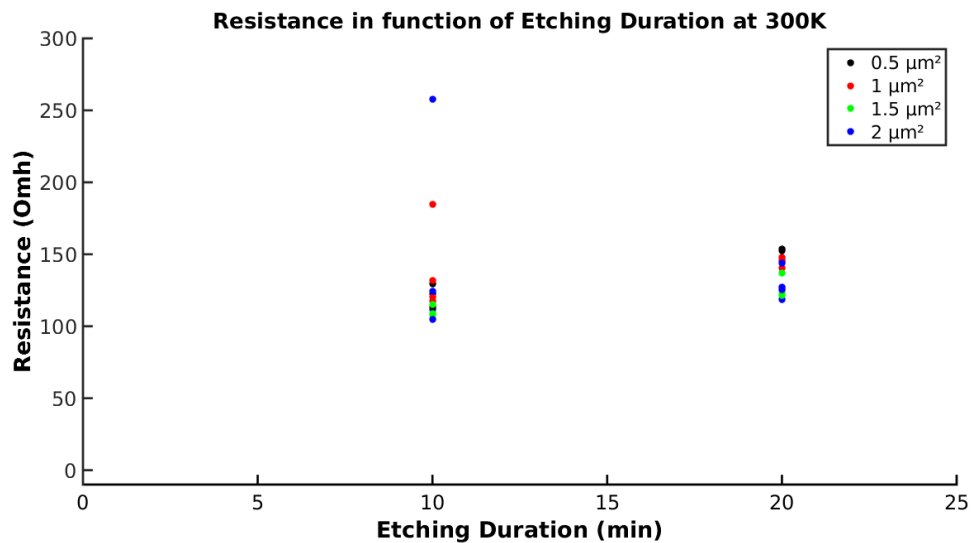
4.2 Low temperature measurements

4.2.1 NIS Junction

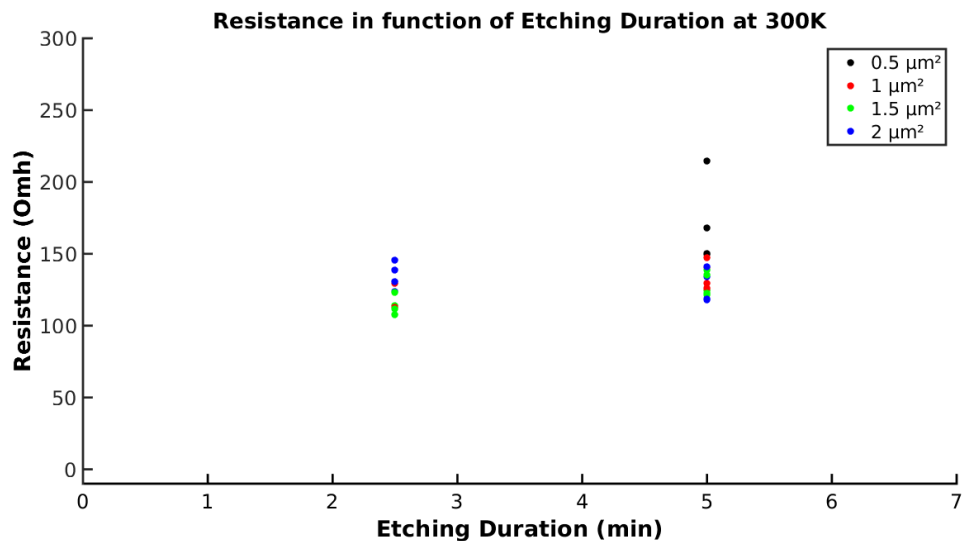
The Figure 4.7a shows the I-V curve that was obtained at low temperature. The curve correspond to what the theory predicts. At a large range of V_{bias} we see almost a strait line : there is tunneling when V_{bias} goes over or under the threshold that the energy gap represents and a flat part in the middle when V_{bias} does not reach the threshold. At a lower range of V_{bias} , closer to the limits of the tunneling, we can see (Fig. 4.7b) better that the flat part is not constant : there is a leakage current, yet the slope is orders of magnitude below the tunneling current. But, there is another phenomenon visible : inside the leakage current there is a part that is steeper, which is the Andreev current, another transport phenomenon [12].

The relation between the tunneling current and the leakage current is about 10^{-4} which is quite good. These results are reproducible between different runs and samples.

Moreover, according to the theory, since the tunneling current is based on the density of states of the two material, if the temperature is modified, the current should be modified. Thermal agitation will have some effects on the I-V curves of the NIS junctions. Indeed, as we can see in Fig. 4.8, the coldest the junction is, the sharper the edges are. Heating will bring electrons in states above the Fermi level, and they will be able to tunnel, even if $|eV| < \Delta$.



(a) Resistance in function of Plasma Etching duration before the cleaning



(b) Resistance in function of Plasma Etching duration after the cleaning

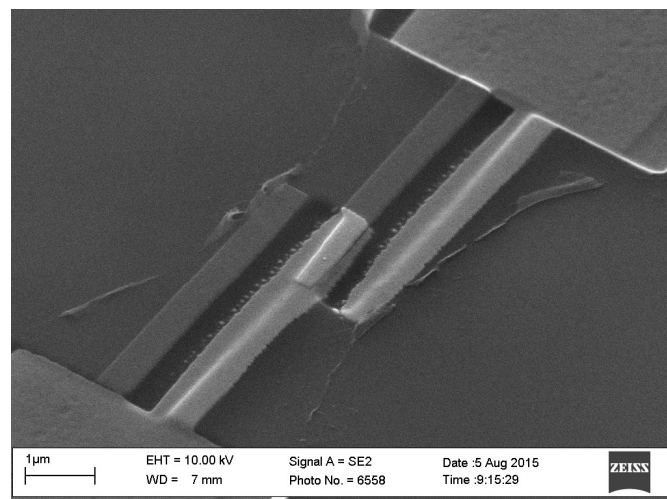
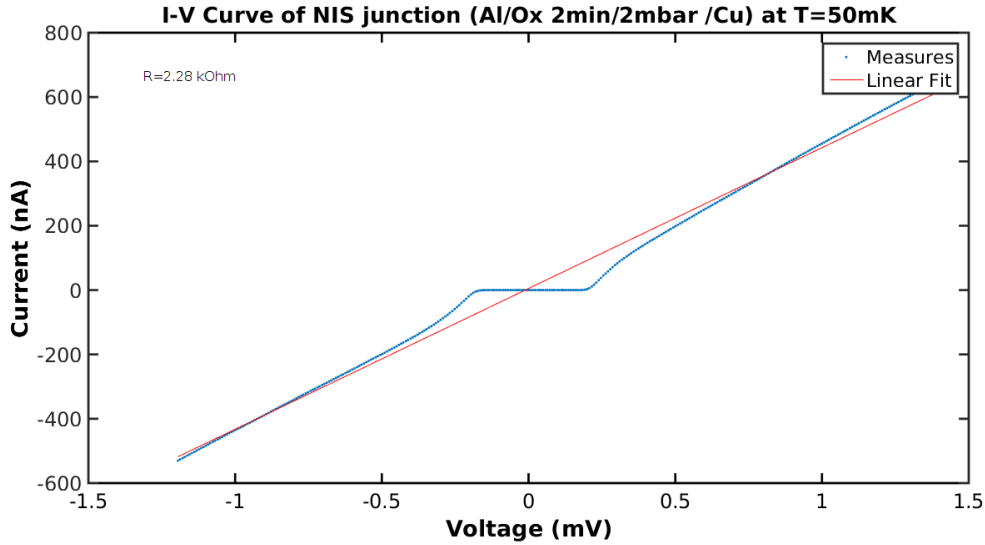
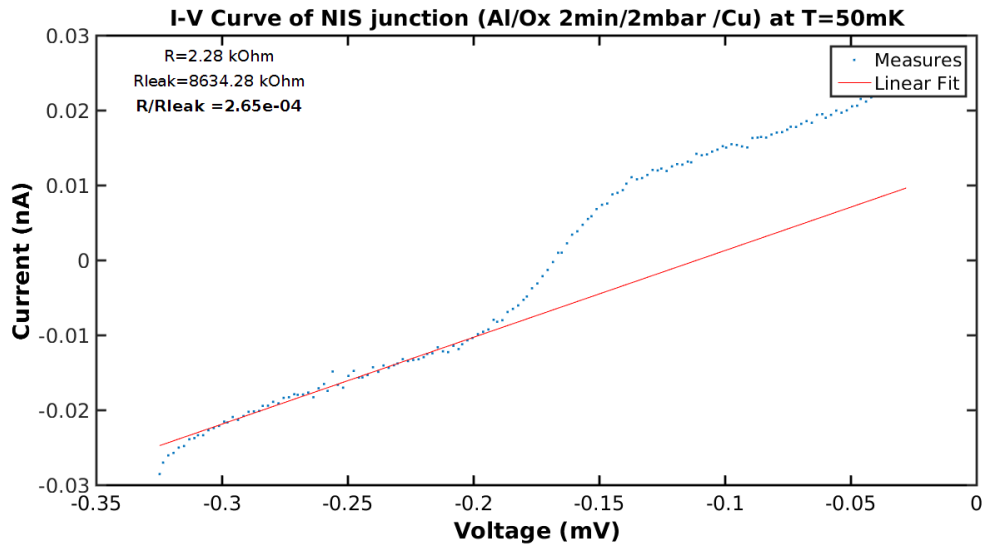


Figure 4.6: SEM Image of a sample where the wafer was etched by plasma



(a) IV curve of NIS junctions with an oxidation under a pressure of 2mbar of O₂ during 2 minutes at 50mK



(b) Zoom in IV curve of NIS junctions with an oxidation under a pressure of 2mbar of O₂ during 2 minutes at 50mK

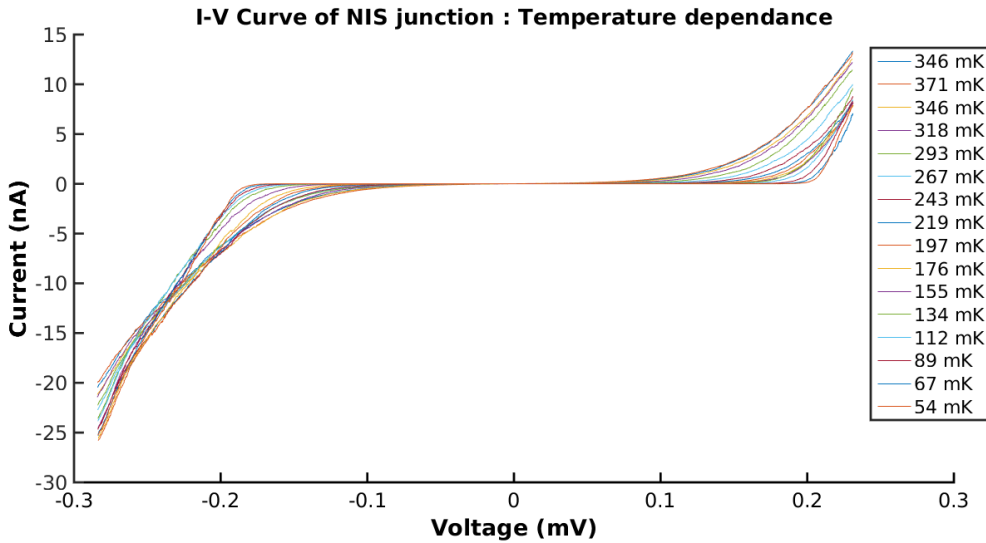


Figure 4.8: Evolution of the IV curves of a NIS junction with the temperature

4.2.2 Plasma etched samples

This part shows the results of the samples where Al was strongly oxidized, then plasma etched and oxidized again to make a tunnel barrier. In order to discriminate the quality of the junctions by themselves, a reference sample was always done at the same time (without plasma etching and with tunnel barrier). Indeed, the junctions can be bad due to external reasons (polluted chamber, bad materials). The Figure 4.9 shows the IV curves which were obtained for a plasma etched sample and the Figure 4.10 show the correspondant regular oxidation reference for this sample.

We can see that the relation between the current is about the same order of magnitude in both cases : 10^{-2} . This is quite a bad result, but since the two relations are about the same value, we could think that the plasma does not damage the junction, but the effect of the plasma etching may be hidden behind the overall poor leakage of all the samples.

4.3 Summary of the results

Plasma etching is working fine, and can etch all the aluminium oxide without any visible damages on the junctions, plus the position of the sample on the sample stage does not affect the behaviour of the plasma etching. The question that has to be solved now is the effect of the plasma on the general quality of the junctions made in the evaporator : after heavy uses of the plasma, the quality of the junctions, in general, have degrading. Is it a coincidence or is it a collateral effect of the plasma ? This has to be solved but still not clear.

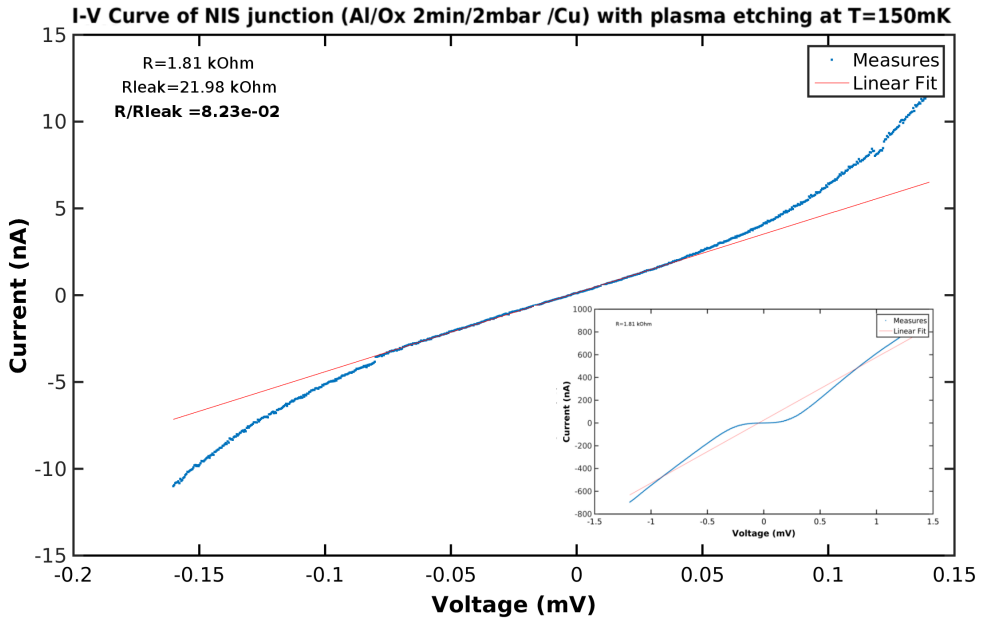


Figure 4.9: IV curves of Plasma Etched sample

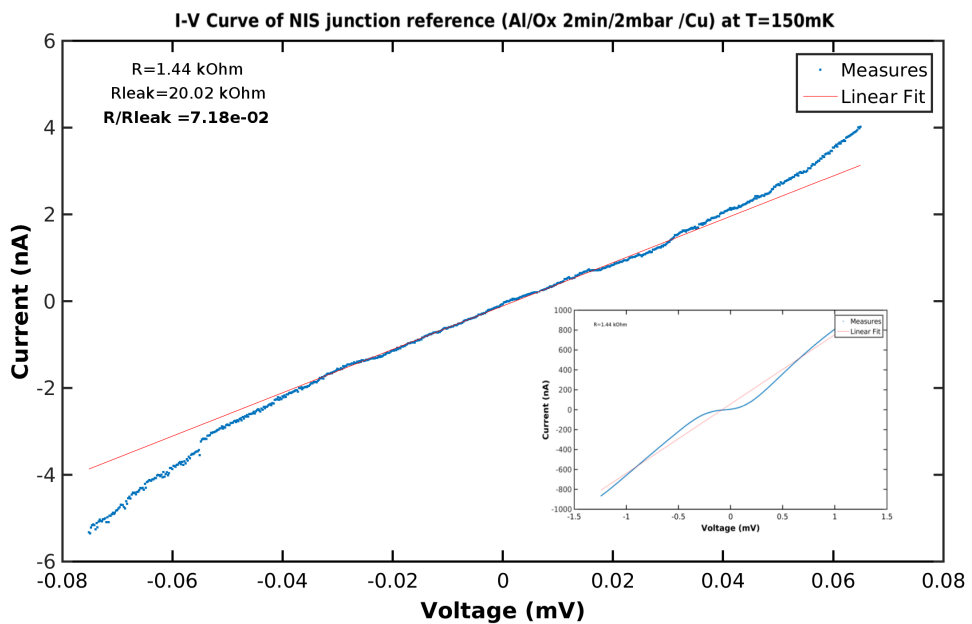


Figure 4.10: IV curves of the reference oxidation sample

Conclusion

In research, it is important to be able to rely on the tools used to fabricate or measure. Manufacturers provide data to give general informations about the tools, yet parameters do not always give the behavior of the tools. This is why characterization of tools is a crucial part of research to have a solid base to start.

The goal of the project was to determine if plasma etching is a reliable method to etch matter *in situ*, since it can be useful for some fabrication processes and so characterize the behavior of the plasma in the evaporator nicknamed LISA, a recent acquisition of the cleanroom.

We first learned about the theoretical background on which the phenomenon rely, to be able to understand what happens. This was possible through a bibliography study on the fields involved. Then, an important part of the project have been devoted to learning and then being able to use the necessary tools in the cleanroom, either the functionning of the tools as the practical use of each one. In the meanwhile, the process was set up, all the settings determined and kept constant to have a reliable and systematic method, punctuated by maintenance interruptions. So, we could make measurements on the structures realized both at room and low temperature because the two of them give different informations about etching. According to the results the measurements gave, plasma etching is a reliable method to etch matter *in situ*. We were able to determine its isotropy on the sample stage and assume that it does not damages the junctions. Yet, we were not able to determine a perfect etching duration, since it seems heavily dependant on the cleanliness of the plasma gun.

However, the results obtained still give important information about plasma etching and can help for future processes that could involve it.

Bibliography

- [1] D. Gobulev and J.P. Pekola. Statistics of heat exchange between two resistors. 2015.
- [2] J.P. Pekola, O.P. Saira, V.F. Maisi, A. Kemppinen, and M. Möttönen. Single-electron current sources: Toward a refined definition of the ampere. *Review of Modern Physics* 85, 2013.
- [3] F. Giazotto, Tero T. Heikkilä, A. Luukanen, A. M. Savin, and J. P. Pekola. Opportunities for mesoscopics in thermometry and refrigeration: Physics and applications. *Rev. Mod. Phys.*, 2006.
- [4] M. Tinkham. *Introduction to Superconductivity*. McGraw Hill, 1996.
- [5] J. Bardeen, L. N. Cooper, and J. R. Schrieffer. Theory of superconductivity. *Phys. Rev.* 108-5, 1957.
- [6] I. Giaever. Energy gap in superconductors measured by electron tunneling. *Phys. Rev. Lett.* 5, 147, 1960.
- [7] R.C. Dynes and J.P. Garno. Tunneling study of superconductivity near the metal-insulator transition. *Phys. Rev. Lett.* 53-25, 1984.
- [8] MicroChem. *NanoPMMA and copolymer*, 2001.
- [9] M.A. Mohammad, M. Muhammad, S.K. Dew, and M. Stepanova. Fundamentals of electron beam exposure and development. *Springer*, 2012.
- [10] J. Muhonen. *Cooling and heat transport in low dimensional phonon systems, superconductors and silicon*. PhD thesis, 2012.
- [11] N. Craig and T. Lester. Hitchhiker's guide to the dilution refrigerator. 2004.
- [12] Ville F. Maisi. *Andreev tunneling and quasiparticle excitations in mesoscopic normal metal – superconductor structures*. PhD thesis, 2014.

Appendix A

Specification about experimental methods

A.1 Chemicals

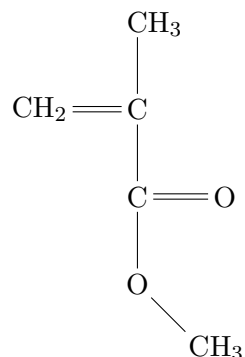


Figure A.1: Chemical structure of MMA, PMMA is a polymer made of this monomer

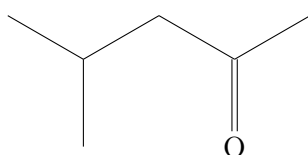


Figure A.2: Chemical structure of MethylIsobutylKetone (MIBK)

A.2 EBL schematics

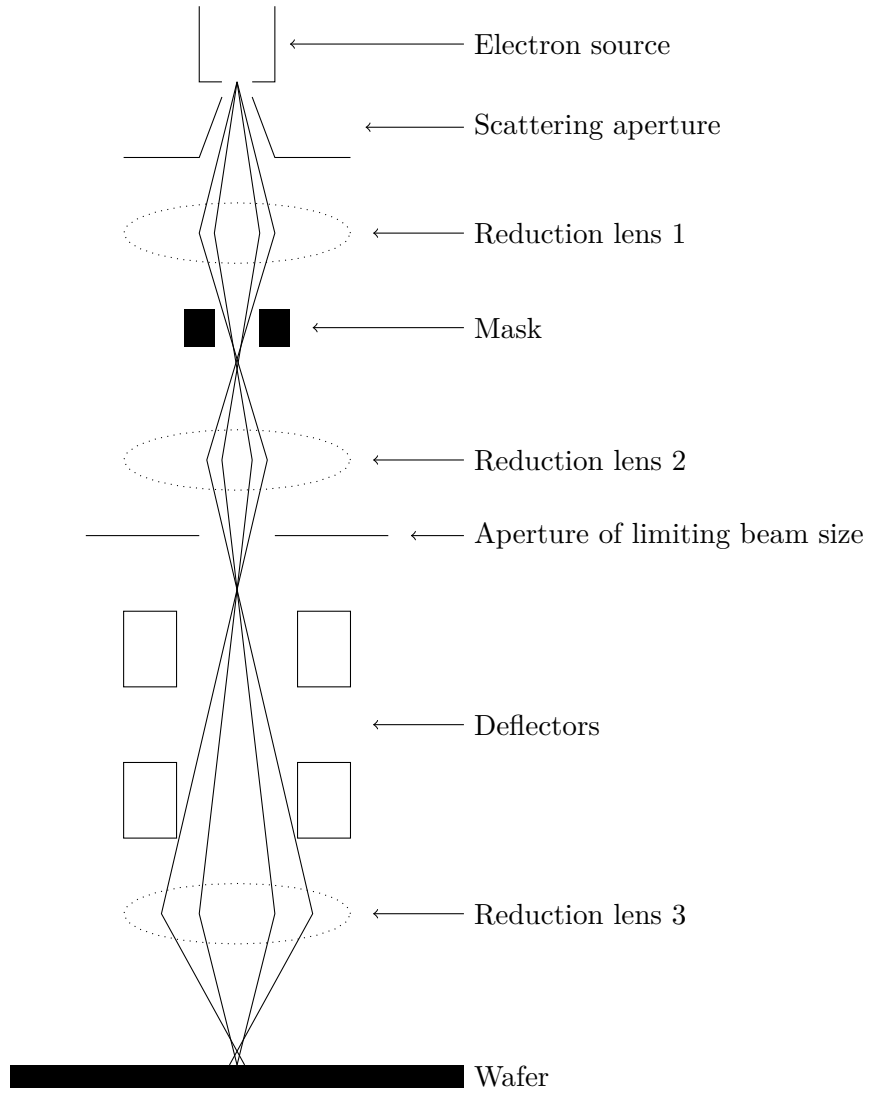


Figure A.3: Simplified EBL functional diagram

Appendix B

Parameters table of the samples

TEST N°	STRONG OXIDATION	PLASMA	REGULAR OXIDATION	COMMENT
Test 10				Failed EBL
Test 11				Failed EBL
Test 12	No	No	No	Clean contact reference
Test 13.i	Yes	10 min	No	Several positions
Test 14.i	Yes	20 min	No	Several positions
Test 15	Yes	No	No	Strong Oxidation reference
Test 16	No	No	Yes	Reference Sample Test 17
Test 17	Yes	10 min	Yes	Resist burned
Test 18	Yes	10 min	Yes	Resist burned
Test 19	No	No	Yes	Reference Sample Test 18
Test 20	Yes	10 min	Yes	Resist burned
Test 21	No	No	Yes	Reference Sample Test 20
Test 22	Yes	5 min	No	
Test 23	Yes	2 min 30s	No	
Test 24	Yes	10 min	Yes	Etched the wafer
Test 25	No	No	Yes	Reference Sample Test 24
Test 26	Yes	2 min	Yes	
Test 27	No	No	Yes	Reference sample Test 26

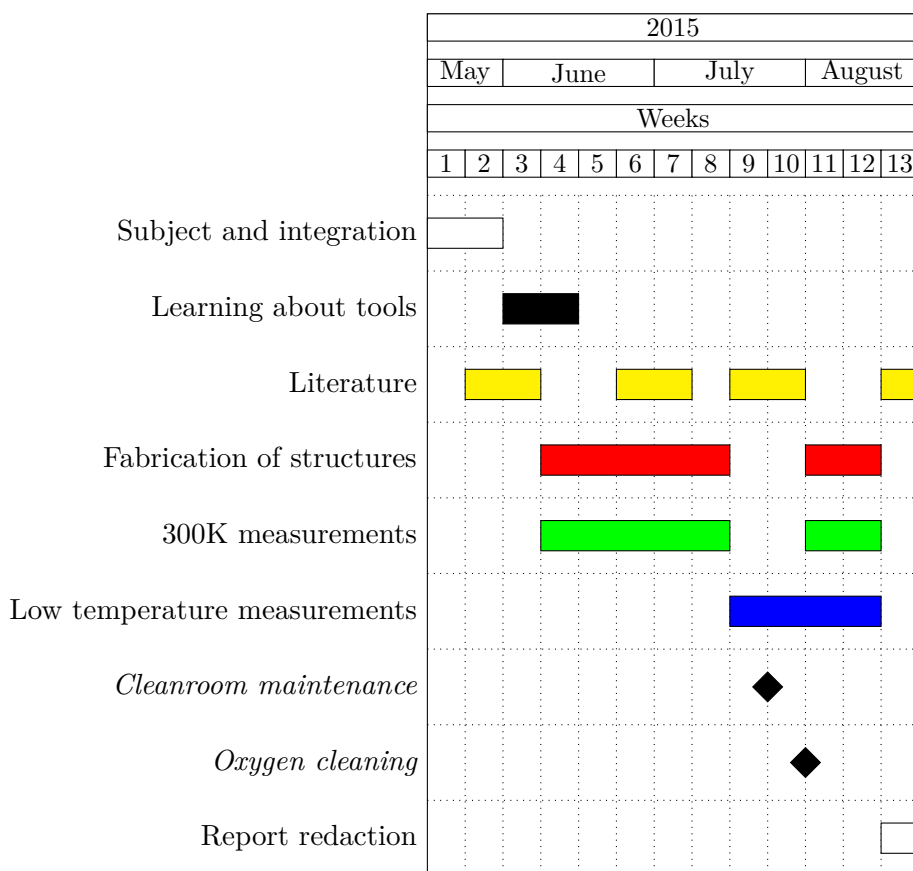
Parameters :

- Pad dimensions : $150 \times 150 \mu m$
- Lead length : $96 \mu m$
- Strong Oxidation = 10 min under a pressure of 200 mbar of O_2
- Regular Oxidation = 2 min under a pressure of 2 mbar of O_2
- Plasma = Pressure of Ar of 4.10^{-4} mbar, Power=40mA, Extraction=-0.8kV¹, Ion Energy=1.5kV

¹Lowered to -0.25kV starting from Test 22

Appendix C

Gantt Diagramm



Abstract

Fabrication and measurements of Normal Metal - Insulator - Superconductor junctions to characterize plasma Etching

The goal of this internship is to characterize an etching method that can be performed *in situ* to get rid of an unwanted layer of matter : Plasma Etching. Thus, a fabrication process was put in place in cleanroom in order to make the structures (Normal Metal - Insulator - Superconductor junctions) to measure. This process relies on several cleanroom methods, but particularly on the evaporator that allows metal deposition and plasma etching. The measurements done are mostly resistance and current-voltage measurements both at room and low temperature, reached with a dilution cryostat. The reference samples consists in simple NIS junctions, without plasma etching shows results expected by theory : surface dependance of resistance, tunnel and leakage current... Results and conclusions about plasma etching were bothered by some parameters modification (Oxygen cleaning of the plasma gun). Yet, it is interesting to notice that plasma etching is a valide etching method since it can etch Aluminium Oxide, which is isotropic on all the sample stage surface and which is does not imply any damages in the junctions. This internship could determine several key data about plasma etching in the evaporator and help researcher with a new and characterized method to etch.

Key words : Plasma Etching, Evaporator, NIS junctions, Low temperature measurements.

Résumé

Réalisation et mesure de jonctions Métal - Isolant - Supraconducteur pour la caractérisation de la gravure par plasma

Le but de ce stage est de caractériser une méthode de gravure permettant de retirer *in situ* une couche de matière non souhaitée : la gravure par plasma. Ainsi, un processus de fabrication a été mis en place afin de réaliser des structures (jonctions Métal-Isolant-Supraconducteur) à mesurer, incluant, ou non (échantillons référence), la gravure par plasma. Il s'appuie sur différentes techniques de salle blanche, en particulier l'évaporateur permettant de déposer le métal mais aussi de graver avec le plasma. Des mesures de résistances et des tracés de caractéristiques courant-tension ont été réalisées, à la fois à température ambiante et à basse température, atteinte par la biais d'un cryostat à dilution. Les échantillons de référence qui consistent en de simples jonctions sans gravure montrent un comportement conforme à celui attendu par la théorie : dépendance en surface de la résistance, courant tunnel et courant de fuite à basse température... Le nettoyage du pistolet à plasma par oxygène a perturbé les résultats concernant la gravure par plasma. Cependant, on notera que le plasma est capable de graver l'Oxyde d'Aluminium, qu'il est isotrope sur l'ensemble du porte-échantillon, et que les jonctions ne sont visiblement pas endommagées par la gravure. Ce stage a donc permis la caractérisation de plusieurs paramètres concernant la gravure par plasma au sein de l'évaporateur et aide à la recherche grâce à cette technique désormais caractérisée.

Mots clés : Gravure par plasma, Evaporateur, Jonctions NIS, Mesures à basse température.